R. & M. No. 3121
(19,030)
A.R.C. Technical Report

MINISTRY OF SUPPLY

AERONAUTICAL RESEARCH COUNCIL
REPORTS AND MEMORANDA

Investigations into the Use of an Electrical Resistance Analogue for the Solution of Certain Oscillatory-Flow Problems

By

P. J. PALMER, ANNE R. COPSON and S. C. REDSHAW,
of the University of Birmingham

LONDON: HER MAJESTY'S STATIONERY OFFICE
1959
PRICE 8*s*. 6*d*. NET

Investigations into the Use of an Electrical Resistance Analogue for the Solution of Certain Oscillatory-Flow Problems

By

P. J. PALMER, ANNE R. COPSON and S. C. REDSHAW,
of the University of Birmingham

Reports and Memoranda No. 3121

February, 1957

Summary.—The use of an electrical resistance analogue, for solving the problem of a thin two-dimensional wing oscillating in an incompressible ideal fluid, is considered; wings with and without flaps are investigated. The particulars of the design and construction of a special graded analogue are given.

Experimental results are obtained for flat plates, with and without flaps, oscillating harmonically with small amplitudes in a steady air stream. These experimental results are in close agreement with theory.

1. *Introduction.*—Electrical resistance analogues have been used successfully to solve many steady-flow problems for aerofoils in both two and three dimensions, the procedure involved being both simple as well as rapid.

The purpose of the present work was to investigate the practicability of using a resistance analogue to determine the aerodynamic forces on a two-dimensional oscillating aerofoil, with and without a flap. This is an appreciably more difficult problem than the steady-flow case, but an electrolytic tank has been used with success for the case of a flat plate with no flap, by Landahl and Stark[1], and by Duquenne[2]. The basic problems for the resistance network are the same as those for the electrolytic tank, but the practical problems are rather different.

The techniques used by Landahl and Stark, and by Duquenne, differ from each other in so far as the electrical potential in the analogue was not equivalent to the same aerodynamic function in both cases.

The procedure described in the present paper is similar to that used by Landahl and Stark, but here not only is a resistance network used instead of a tank, but the work is extended to aerofoils with flaps.

In all the procedures referred to above, the solution of the oscillatory-flow problem is reduced to the solution of some equivalent steady-flow problems.

2. *Basic Mathematical Problem.*—For the case of a thin two-dimensional wing oscillating in a steady air stream in an incompressible medium, where the oscillations are small, the problem can be represented by Laplace's equation, which is satisfied by both the velocity potential Φ and the acceleration potential ϕ, i.e.,

$$\frac{\partial^2 \Phi}{\partial x^2} + \frac{\partial^2 \Phi}{\partial z^2} = 0$$

$$\frac{\partial^2 \phi}{\partial x^2} + \frac{\partial^2 \phi}{\partial z^2} = 0 ,$$

where the x axis is parallel to the air stream and the z axis is normal to it.

The mean position for the aerofoil is taken as the x axis, and since the amplitude of the deflections are small, the corresponding boundary conditions are actually applied on this axis.

If the oscillations are harmonic with frequency ν, the above functions can be represented by

$$\Phi(x, z, t) = \bar{\Phi}(x, z)\, e^{i\nu t}$$
$$\phi(x, z, t) = \bar{\phi}(x, z)\, e^{i\nu t},$$

the velocity components due to the perturbation being obtainable in the usual way by differentiation.

A third potential function satisfying Laplace's equation is

$$\psi(x, z) = \frac{1}{U^2} \int_{\xi=-\infty}^{\xi=x} \bar{\phi}(\xi, z)\, d\xi\ ,$$

where U is the free-stream velocity. This function was proposed by Landahl and Stark and used by them in the solution of the problem, whereas Duquenne used the velocity potential.

Broadly speaking, the problem could be solved in terms of any one of these three functions, but the practical problems are different for each case. The acceleration potential ϕ would involve difficulties associated with singularities and also, as with steady-flow problems, the aerofoil incidence could not be determined prior to the experiment. The velocity potential Φ involves carrying out separate experiments for each value of the frequency, and also the boundary conditions are difficult; this procedure was used by Duquenne. The potential function ψ entails one set of experiments with simple boundary conditions independent of the frequency, but the subsequent numerical work involves difficulties associated with the integration. However, this latter method is the one adopted by Landahl and Stark and also it is the one chosen by the present authors as being the most convenient.

3. *Boundary Conditions.*—The boundary conditions of the problem in terms of the potential function ψ, can be expressed very simply, except over the aerofoil.

In the plane x, z, with the leading edge of the aerofoil at $x = 0$ and the trailing edge at $x = c$, these boundary conditions are as follows:

(1) $\psi(x, z)$ is an odd function of z

(2) $\psi(x, 0) = 0$ for $x \leqslant 0$

(3) $\psi(x, 0) = \psi(c, 0)$ for $x > c$

(4) $\psi(x, z) \to 0$ as $x \to -\infty$ and $z \to +\infty$

(5) *For* $0 < x < c$; $z = 0$

$$\psi_z(x, 0) = \frac{\bar{w}}{U} + \frac{i\nu}{U^2} \int_0^x \bar{w}(\xi)\, d\xi + \frac{i\nu}{U} \int_{-\infty}^0 \psi_z\, e^{i\nu\xi/U}\, d\xi\ ,$$

in which

$$w = \bar{w}\, e^{i\nu t},$$

where w is the velocity normal to the free air-stream direction, i.e., $z = 0$. Thus, if the wing position at any time t is given by $z = f(x)\, e^{i\nu t}$, then $\bar{w} = U f_x(x) + i\nu f(x)$. The boundary conditions referred to above are self-explanatory except for the last one, which gives the normal gradient to be applied over the wing.

This condition can be written as

$$\psi_z(x, 0) = \psi_z^{(1)}(x, 0) + \psi_z^{(2)}$$

where

$$\psi_z^{(1)}(x, 0) = \frac{\bar{w}}{U} + \frac{i\nu}{U^2} \int_0^x \bar{w}(\xi)\, d\xi$$

$$\psi_z^{(2)} = \frac{i\nu}{U} \int_{-\infty}^0 \psi_z^{(1)} e^{i\nu\xi/U}\, d\xi + \frac{i\nu}{U} \int_{-\infty}^0 \psi_z^{(2)} e^{i\nu\xi/U}\, d\xi\ .$$

Now $\psi_z^{(1)}$ can be evaluated, split into real and imaginary parts and the corresponding experiments carried out, yielding $\psi^{(1)}$. As a result of these experiments the first term in the expression for $\psi_z^{(2)}$ can be evaluated and then this expression becomes a linear one in $\psi_z^{(2)}$, where $\psi_z^{(2)}$ over the aerofoil is independent of x. Here, generally speaking, by considering real and imaginary parts, one further experiment yields $\psi^{(2)}$. Thus ψ can be determined everywhere. In actual fact, by suitably arranging the experiments to be done, three in number are sufficient for the flat plate, and one of these will yield $\psi^{(2)}$ for other aerofoils, when $\psi^{(1)}$ has been determined.

4. *Resistance-Analogue Arrangement.*—It was decided that, in order to be able to set accurately the required variation of ψ_z over the aerofoil, it would be necessary to provide a fine mesh on the analogue, at least in the vicinity of the aerofoil. Representation of the aerofoil by means of twenty discrete points seemed feasible, and these points correspond to the nodes (pins) of the resistance network. At the same time, the analogue field must be large so that the edge effects are negligible.

Thus, either a very large network with a very fine mesh separation would be required, or alternatively, a graded network could be used, the advantage of the latter being that it is more economical to build. Several analogue network boards were available but none was quite suitable and so a large graded analogue was devised and constructed using the technique developed by Redshaw[6]. This large graded analogue actually consisted of eight separate networks which could be assembled together in a variety of ways to suit the individual applications. Some of these constituent net works were uniform, some graded in one direction and some in two directions. The overall result was that in effect the aerofoil chords were represented by twenty ordinates in a total field measuring 26×21 aerofoil chords. The whole arrangement was very accurate and a photograph of the complete equipment is given in Fig. 1 and the diagrammatic set-up is shown in Fig. 2.

Full details of the design and construction of the analogue are given in Appendix A.

The electrical potential on the resistance board is analogous to the special potential function and is therefore proportional to it. Hence, when ψ itself was specified at the boundary, the proportional electrical potential was set. When ψ_z, the normal gradient, was specified, the corresponding electrical gradient was known. To set this value the boundary potential itself was adjusted and the gradient calculated from the boundary potential and the potentials at the next two positions inwards, normal to the boundary. The three-ordinate technique was used as described by Palmer and Redshaw[3] elsewhere.

A good estimate of the likely accuracy achieved by means of this representation is given by the experiments recorded in Appendix B, where the accuracy of some simple steady-state solutions is considered; the error in the steady-state lift coefficient for a flat plate is only 1 per cent.

5. *Solutions.*—Several examples have been evaluated, including aerofoils both with and without flaps, and the experimental results have been compared with theory.

The first set of examples are concerned with a flat plate oscillating both in pitch and vertical translation. These experimental results have been evaluated for a wide range of frequencies and the results compared with the values calculated by Minhinnick[4, 5]. Fig. 3 gives the results for pitch about the leading edge and Fig. 4 gives the results for vertical translation; the full line on the graphs being the theoretical values from Minhinnick. Both real and imaginary parts are plotted, so that both amplitude and phase can be deduced if required.

For aerofoils with flaps, the case of a flap oscillating about a hinge at its leading edge is considered. The experimental results together with the theoretical values are recorded in Figs. 5 and 6. Fig. 5 gives the case of a flap of 25 per cent chord and Fig. 6 gives the case of a flap of 30 per cent chord.

The pitching moments for the above cases are given in Figs. 7 to 10 inclusive.

In all examples it should be particularly noted that the agreement between experiment and theory is good, even up to the relatively high frequencies considered.

It should be emphasised that the discrepancy between the theoretical results and those deduced from the experiments, is certainly not all due to the inaccuracies of the board itself. Although some of this discrepancy will be associated with the 'fineness' of the mesh, it is considered that most of the discrepancy can be associated with the method of evaluation of the results from the experiments since this process involves approximations. It has been calculated that these approximations can be varied to some extent and hence slightly change the overall results. This aspect is not regarded as being particularly important as the main object of this report is to show the manner in which a resistance analogue can be used to solve oscillatory-flow problems.

Details of the procedure for calculating the relevant data from the experimental results are given in Appendix C.

6. *Conclusion.*—This report shows how an electrical resistance analogue can be used to solve the problem of a thin two-dimensional wing, with and without a flap, oscillating in an ideal incompressible fluid.

A resistance network with a fine mesh separation is required.

Experiments have been carried out using the technique and equipment proposed and, for the cases considered, a good degree of accuracy was obtained.

REFERENCES

No.	*Author*	*Title, etc.*
1	M. T. Landahl and V. J. E. Stark	An electrical analogy for solving the oscillating-surface problem for incompressible nonviscid flow. K.T.H. Aero. T.N.34 (Sweden). July, 1953.
2	R. Duquenne	Étude analogique des ailes en régime instationnaire. Actes des Journées Internationales de Calcul Analogique, Bruxelles. pp. 317 to 321. 1955.
3	P. J. Palmer and S. C. Redshaw..	Experiments with an electrical analogue for the extension and flexure of flat plates. *Aero. Quart.*, Vol. VI, pp. 13 to 30. February, 1955.
4	I. T. Minhinnick	Tables of functions for evaluation of wing and control-surface flutter derivatives for incompressible flow. R.A.E. Report Struct. 86. A.R.C. 13,730. July, 1950.
5	I. T. Minhinnick	Subsonic aerodynamic flutter derivatives for wings and control surfaces (compressible and incompressible flow). R.A.E. Report Struct. 87. A.R.C. 14,228. July, 1950.
6	S. C. Redshaw	A resistance network of novel construction for solving certain problems in elasticity. Actes des Journées Internationales de Calcul Analogique, Bruxelles. pp. 406 to 409. 1955.

(74988) A*

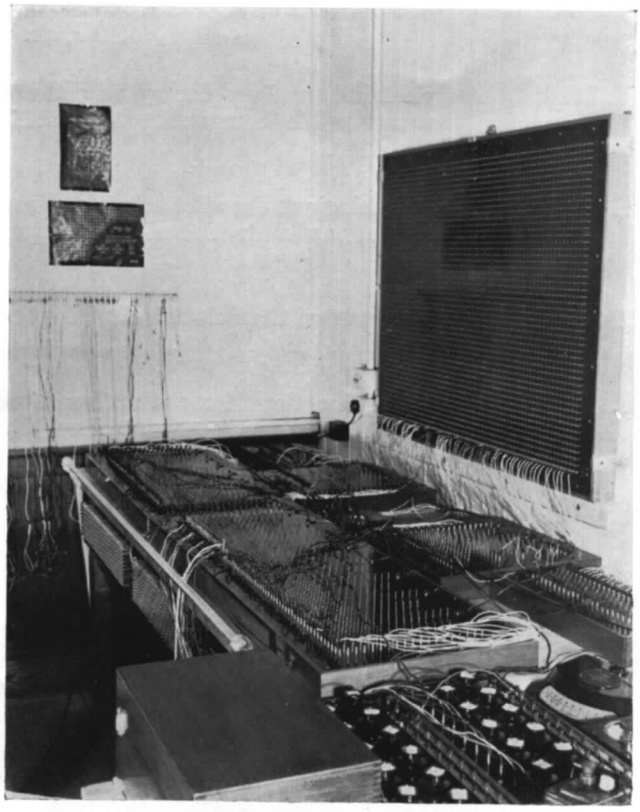

FIG. 1. General view of electrical resistance analogue.

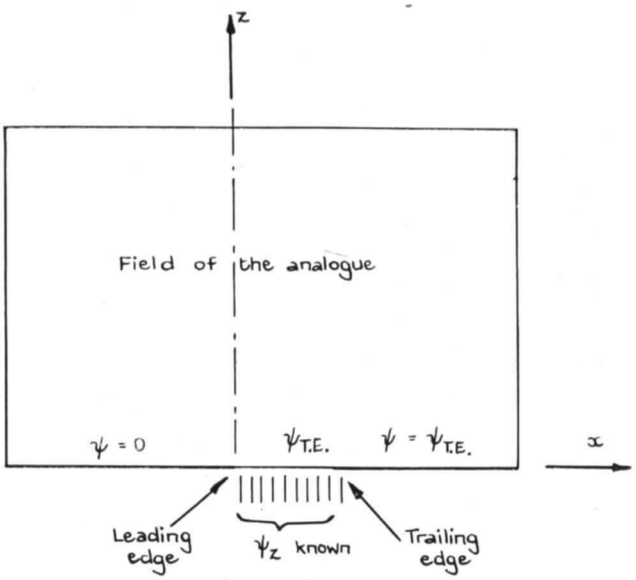

FIG. 2. Diagrammatic representation of the boundary conditions.

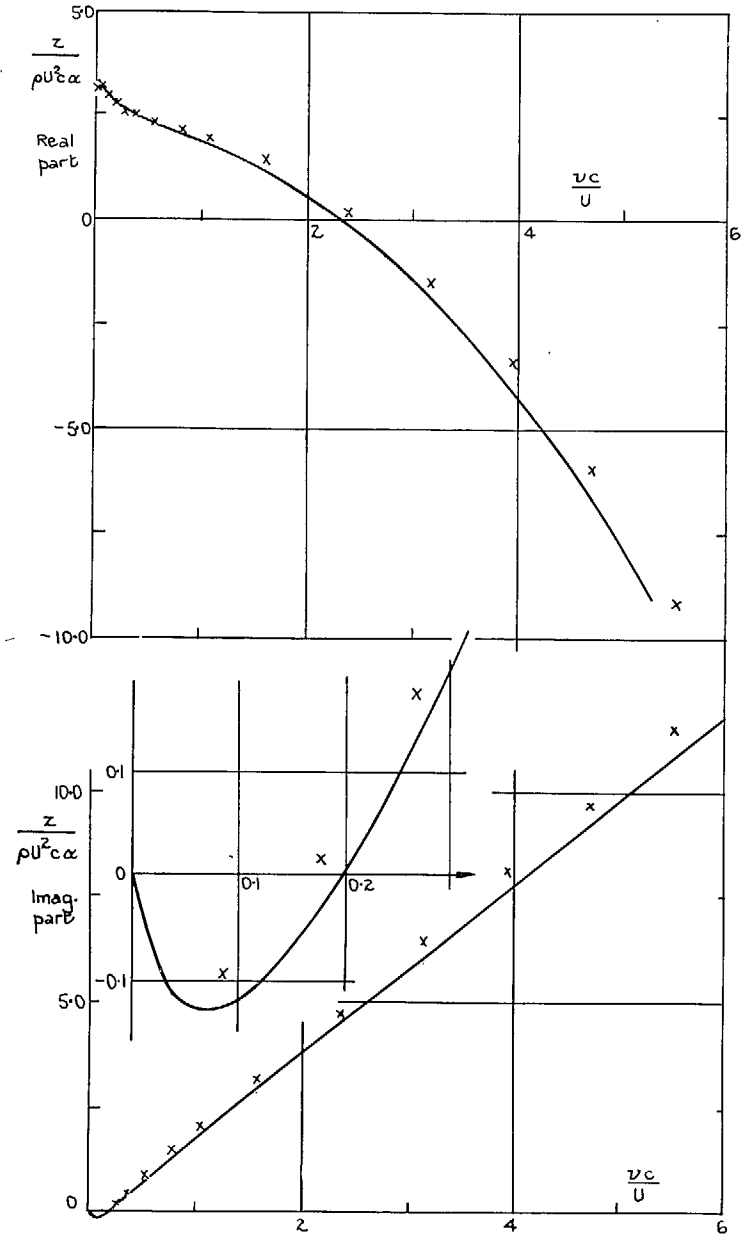

FIG. 3. Flat plate.—Pitch.

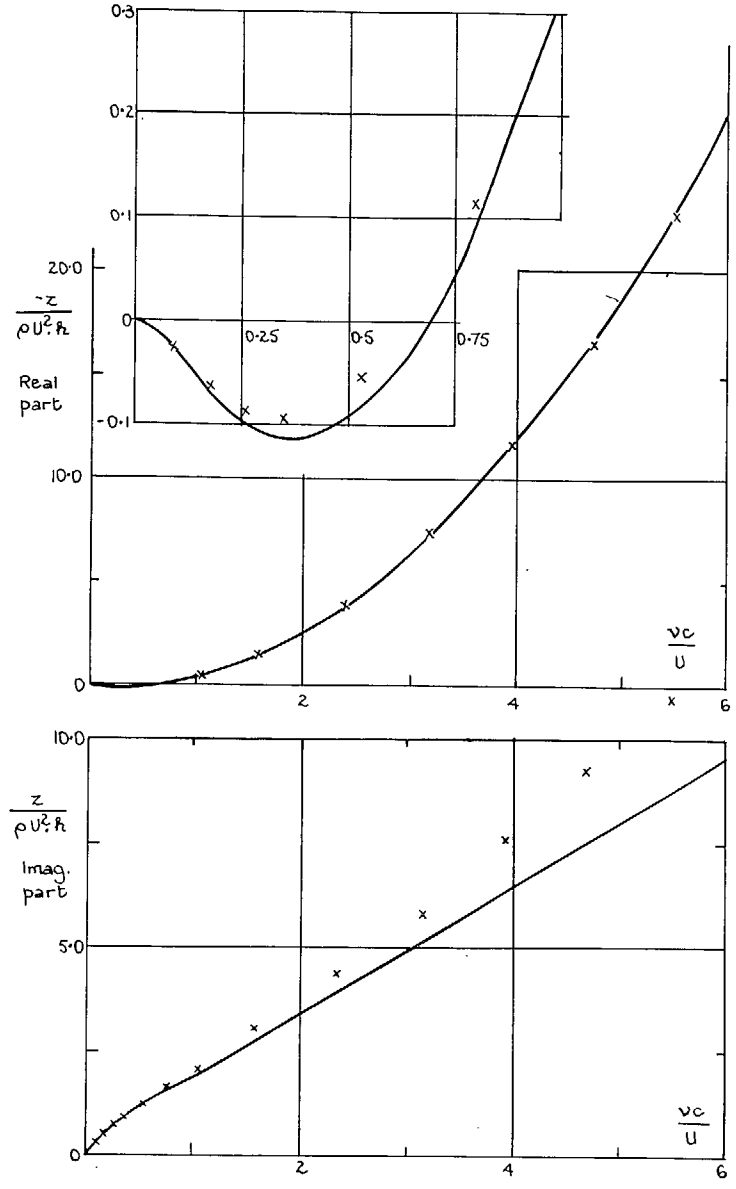

FIG. 4. Flat plate.—Translation.

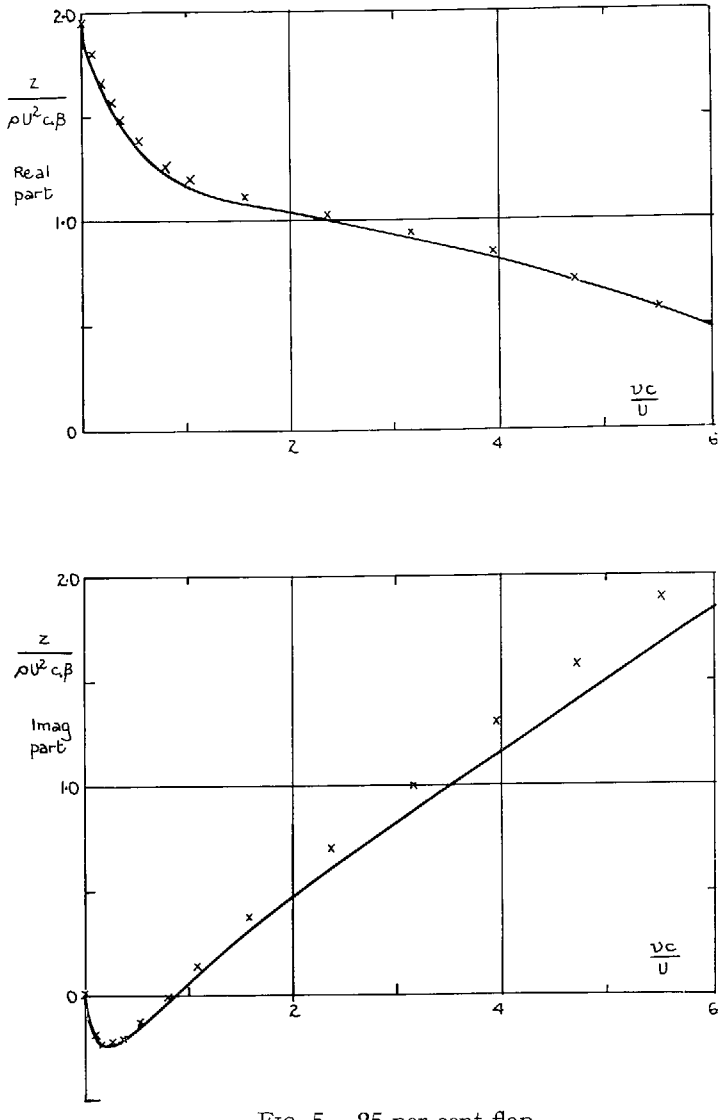

FIG. 5. 25 per cent flap.

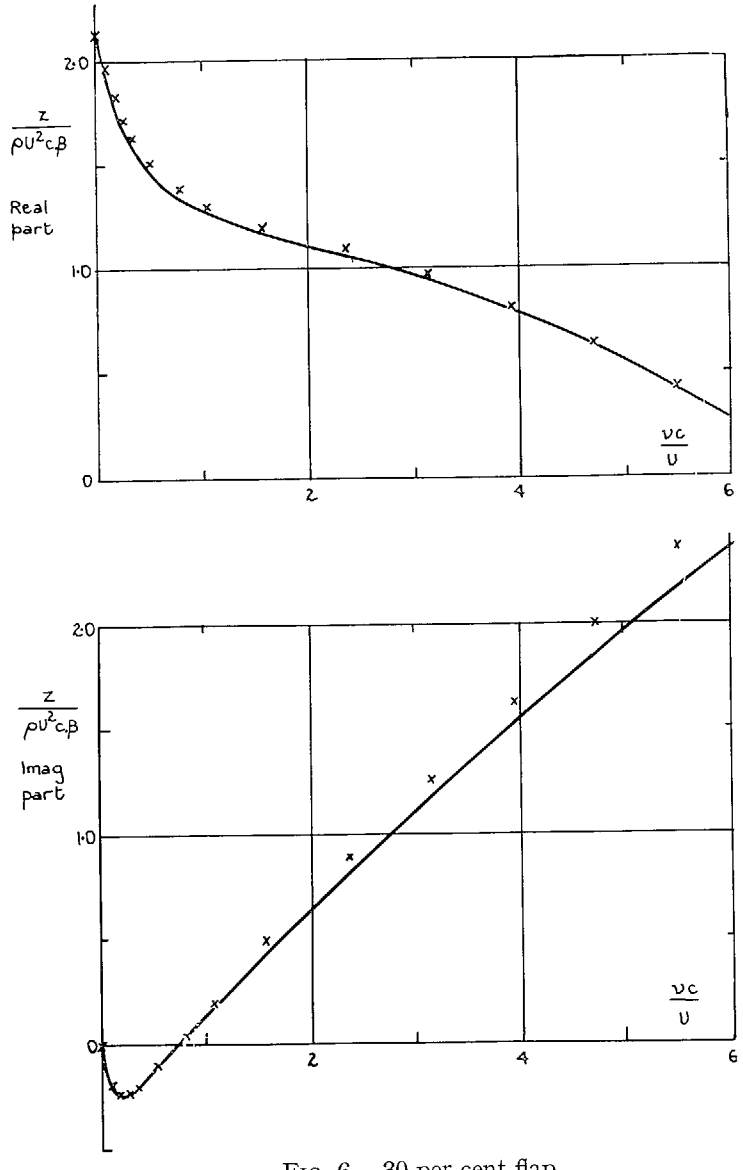

FIG. 6. 30 per cent flap.

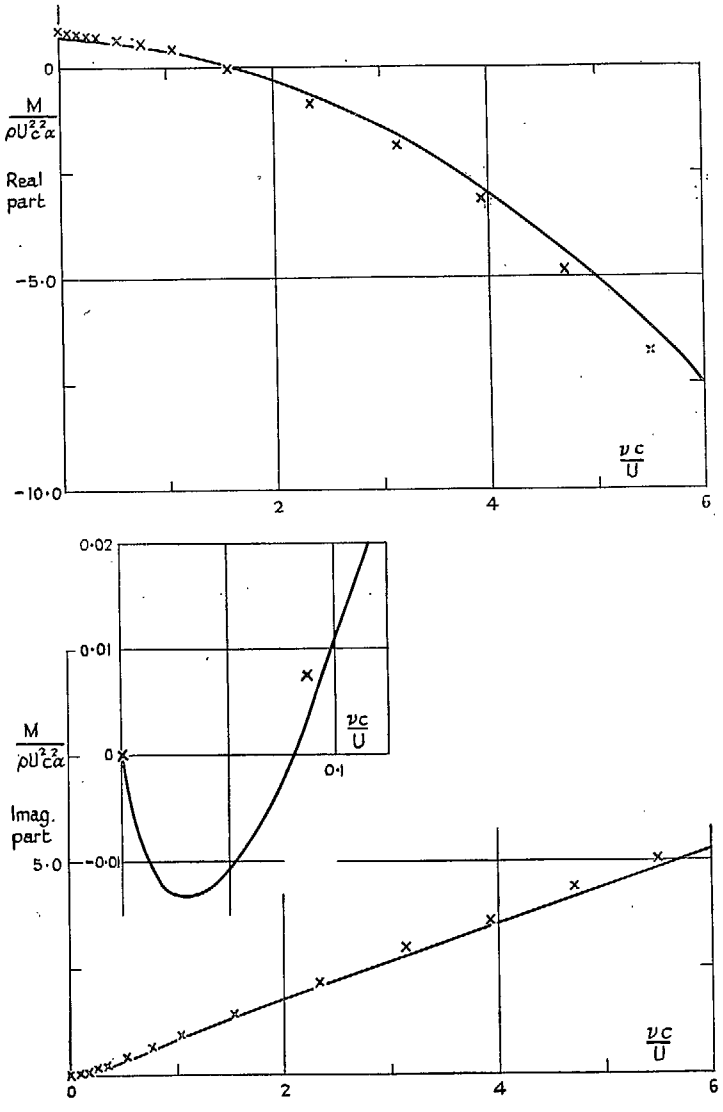

FIG. 7. Flat plate.—Pitch.

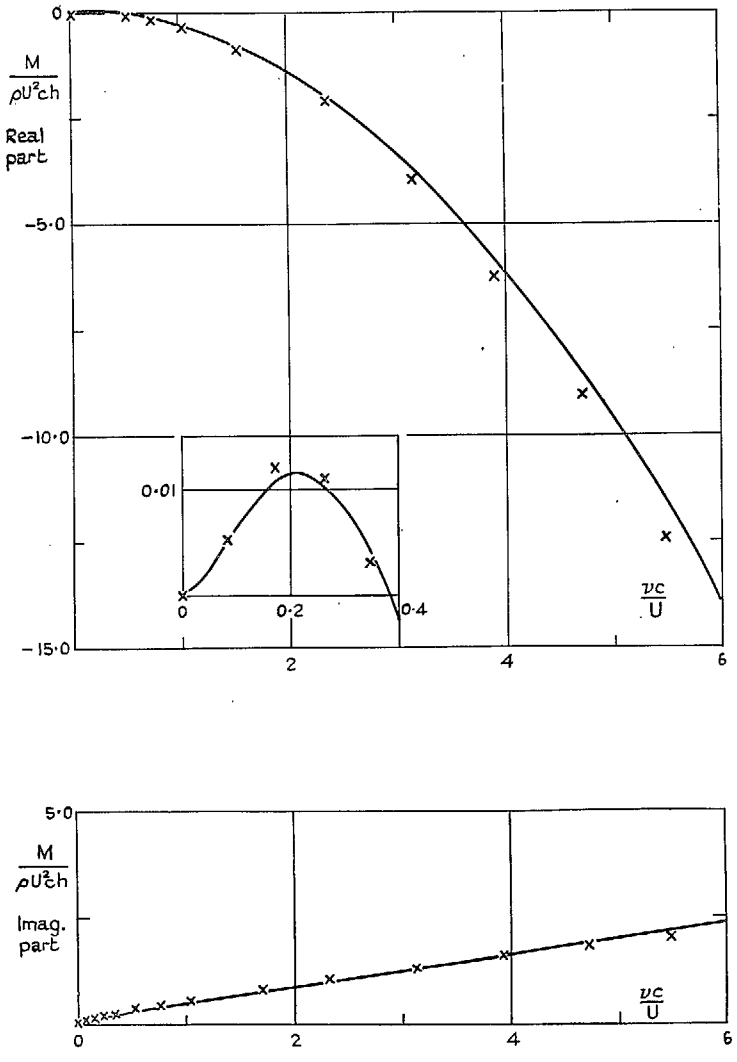

FIG. 8. Flat plate.—Translation.

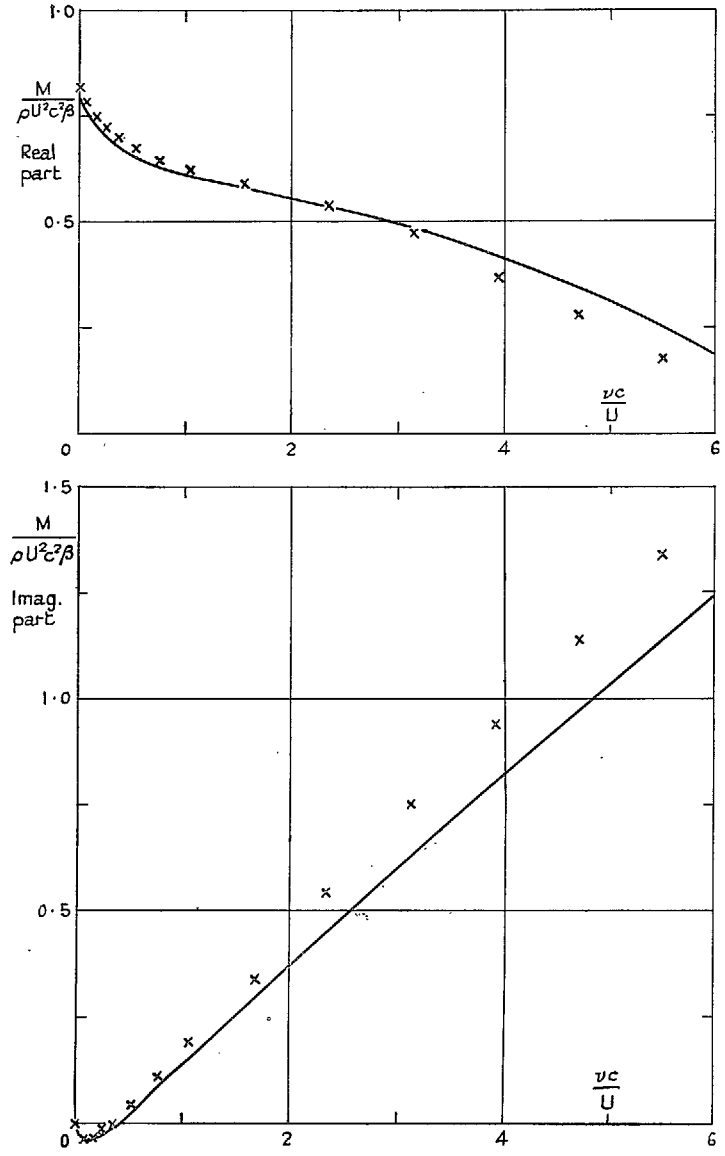

FIG. 9. 25 per cent flap.

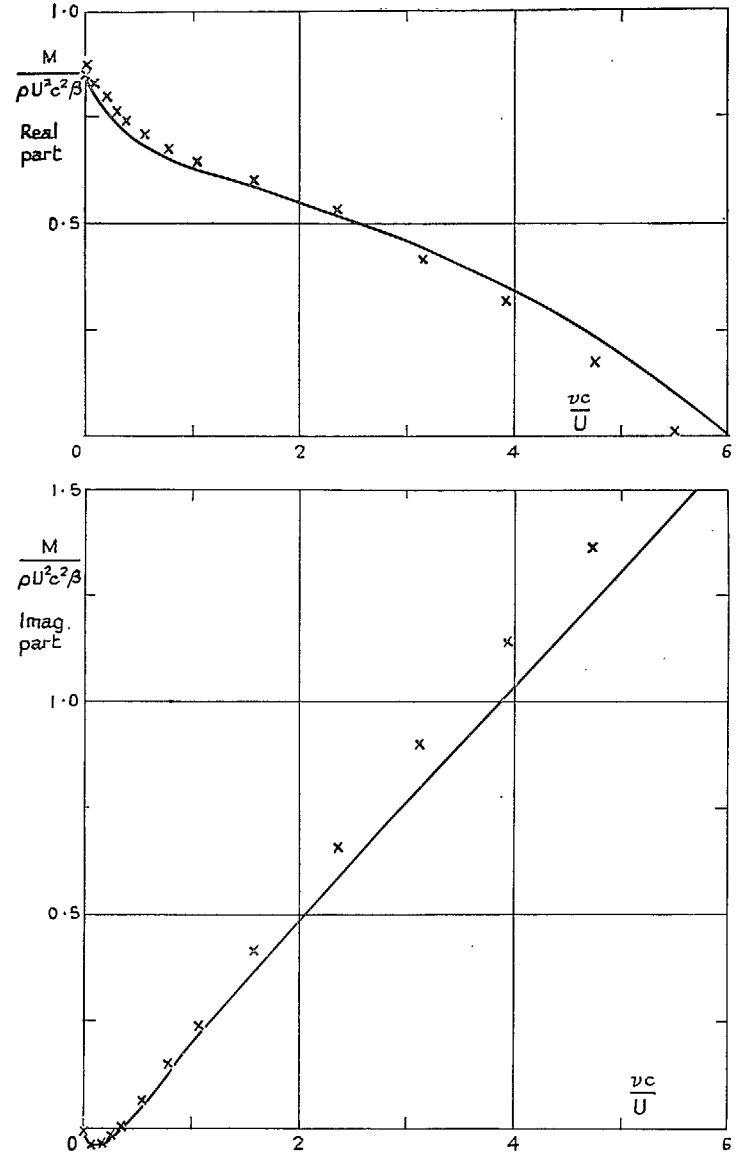

FIG. 10. 30 per cent flap.

APPENDIX A

The Graded Electrical Resistance Analogue.—Design and Construction

1. *Introduction.*—The immediate purpose of the graded electrical resistance analogue was to provide a potential analyser with a fine mesh in that part of the field where, for aerodynamic problems, the aerofoil would be represented. In addition, it was desirable to have the graded parts of the network as standard items so that they could also be readily adaptable for other types of problems. Generally, this means that a graded network may be required to produce a finer mesh separation along one or more edges of a uniform network (as in the present problem), or alternatively, to provide a coarser mesh separation along one or more edges of a uniform network.

The existing uniform network had a mesh separation of 1/64 by 1/48 and was composed of 100-ohm high-tolerance resistance ribbon with a 200-ohm boundary, the construction being described elsewhere by Redshaw[1]. Consequently the graded networks were designed to be used in conjunction with this existing network, and it was decided that it would be necessary to decrease the mesh separation to 1/8th of the uniform-network mesh size.

2. *The Resistance Grading.*—Various types of resistance grading can be devised and used, but that shown in Fig. A.1a was considered to be the most suitable. The desired characteristics were that the graded network should give an accurate finite-difference representation of Laplace's equation and that it should be simple to manufacture. In particular, it should be noted that all the resistors required, in this chosen grading, are in fact either equal to one resistance value or to double this value.

Other gradings, for finite-difference representation, have been devised by MacNeal[2] and by Liebmann[3], but the grading given in this report is as accurate as any and has the advantage that it is readily adaptable to the constructional techniques developed by Redshaw[1,4]. In the present example, to make full use of this technique, the network is not built to a true physical scale but to a distorted scale as shown in Fig. A.1b.

3. *The Mathematical Accuracy of the Chosen Resistance Grading.*—It is well known that the relationship between the electrical potentials at the nodes of a square resistance grid, of side a with all resistances equal and axes x and z, is

$$V_{x+a,\,z} + V_{x,\,z+a} + V_{x-a,\,z} + V_{x,\,z-a} - 4V_{x,\,z} = 0\,.$$

Furthermore, the finite-difference representation of Laplace's equation

$$\frac{\partial^2 \chi}{\partial x^2} + \frac{\partial^2 \chi}{\partial z^2} = 0$$

on a similar grid is

$$\chi_{x+a,\,z} + \chi_{x,\,z+a} + \chi_{x-a,\,z} + \chi_{x,\,z-a} - 4\chi_{x,\,z} = 0\,,$$

provided that terms involving fourth and higher-order differentials are neglected.

These relationships show the harmonic function, contained in Laplace's equation, and the electrical potential, given by a potential analyser with uniform mesh and equal resistances, to be analogous.

Similar relationships for the nodes in a non-uniform, or graded, network exist but these will not necessarily be quite as accurate as those in a uniform network. However, the accuracy of the present network is sufficient and is in fact as high as can be achieved with such simple gradings.

With reference to Fig. A.1a, the errors at the nodes, up to and including third-order differentials, are as given below:

Node	Error
A	$\left\{-a^2\frac{\partial^2}{\partial x\,\partial z}+\frac{a^3}{2}\left(-\frac{\partial^3}{\partial x^3}+\frac{\partial^3}{\partial z^3}-\frac{\partial^3}{\partial x^2\,\partial z}+\frac{\partial^3}{\partial x\,\partial z^2}\right)\right\}\chi_A$
B	$\left\{-\frac{a^2}{4}\left(\frac{\partial^2}{\partial x^2}-\frac{\partial^2}{\partial z^2}\right)-\frac{a^3}{2}\left(\frac{\partial^3}{\partial x^2\,\partial z}-2\frac{\partial^3}{\partial z^3}\right)\right\}\chi_B$
C	$\left\{+\frac{a^3}{2}\left(\frac{\partial^3}{\partial x^2\,\partial z}-\frac{\partial^3}{\partial x\,\partial z^2}\right)\right\}\chi_C$
D	0
E	$\left\{+\frac{a^2}{4}\left(\frac{\partial^2}{\partial x^2}-\frac{\partial^2}{\partial z^2}\right)+\frac{a^3}{2}\left(\frac{\partial^3}{\partial x^2\,\partial z}\right)\right\}\chi_E$

In particular it should be noted that the nodes B and E, which constitute the vast majority of nodes in a graded network, are self compensatory as regards the second-order errors.

From the above Table there are no first-order differential errors. Hence, provided that the potential gradient is approximately constant over the actual graded portion of the network, high accuracy can be achieved.

4. *The Method of Construction.*—The method of construction was basically that described by Redshaw[1], except that for graded networks the resistance ribbons were not placed diagonally but were placed in both the x and z directions. To avoid electrical shorting, the resistance ribbons were placed between transparent insulation tape before assembly.

The grading to 1/8th of the original mesh size was carried out in three stages and this meant that, by building the units to the distorted scale shown in Fig. A.1b, only eight different types of resistance ribbon were required. Some of these ribbons had loops for soldering on both sides, some only on one side, and also the loop spacing varied. The resistance between consecutive loops was 100 ohms for some ribbons and 200 ohms for the others, with a maximum tolerance of $\pm$ 1 per cent. The advantage of the distorted scale was principally that it permitted longer lengths of ribbon, with uniform resistance per unit length, to be assembled in one operation than would otherwise be possible. It should be remembered that the resistance per unit square of a conducting sheet is independent of the size of the square ; similarly, the resistances in the uniform parts of a network are independent of the size of the mesh.

Photographs of a graded resistance analogue are given in Figs. A.2a and A.2b. The first Figure shows the front view of the board and the second the rear view. In this case grading is carried out in both directions, the board forming a 'corner' graded resistance unit.

As in the case of the uniform boards, the whole assembly is encapsulated in resin on completion.

5. *The Various Units and the Possible Arrangements.*—In all, some eight boards constituted the units for making up the complete graded networks. Three of these were uniform, three graded in only one direction, and two graded in both directions.

The particulars of these boards are given below:

Board	Type	Size	Number available
A	Uniform	64 × 48 units	1
B	Uniform	5 × 20 units	2
C	Graded in one direction	Graded from 8 to 64 units .. .. Effectively 5 × 8 units (coarse units)	1
D	Graded in one direction	Graded from 6 to 48 units .. .. Effectively 5 × 6 units (coarse units)	2
E	Graded in two directions	Effectively 5 × 5 units (coarse units)	2

The details of the gradings used are given in Fig. A.3. These sketches are drawn to the distorted scale to which they were constructed. The effective scale is shown on the drawings.

The two principal methods of joining these units together are shown in Fig. A.4. The first method gives a fine mesh along one side of the board over a limited region. This method is very useful for aerofoil applications and gives an effective mesh separation over the aerofoil of 1/424 by 1/512. The second method gives a coarse grading over three sides of the board, so that the effective size of the main board is increased and the mesh separation therefore effectively reduced to 1/144 by 1/88.

Other methods of assembly for the various units can be devised but the two arrangements shown here serve to illustrate the technique.

REFERENCES.—APPENDIX A

No.	*Author*	*Title, etc.*
1	S. C. Redshaw	A resistance network of novel construction for solving certain problems in elasticity. Actes des Journées Internationales de Calcul Analogique, Bruxelles. pp. 406 to 409. 1955.
2	R. H. MacNeal	An asymmetrical finite difference network. *Quart. App. Math.* Vol. XI. No. 3. pp. 295 to 310. October, 1953.
3	G. Liebmann	Resistance-network analogues with unequal meshes or sub-divided meshes. *Brit. J. App. Phys.* Vol. 5. No. 10. pp. 362 to 366. October, 1954.
4	S. C. Redshaw	A three-dimensional electrical potential analyser. *Brit. J. App. Phys.* Vol. 2. No. 10. pp. 291 to 295. October, 1951.

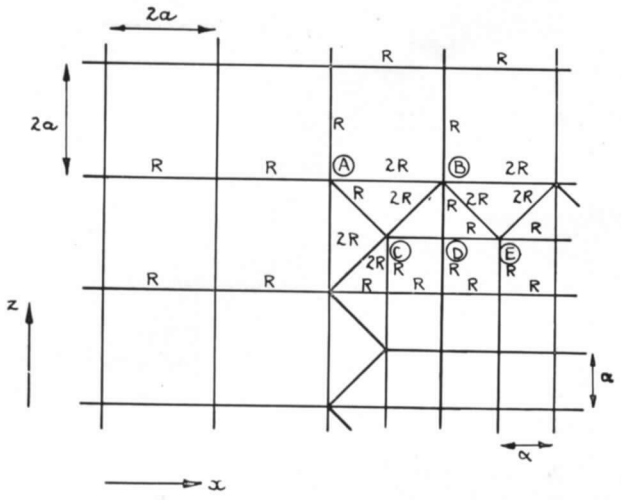

(a) Natural scale.

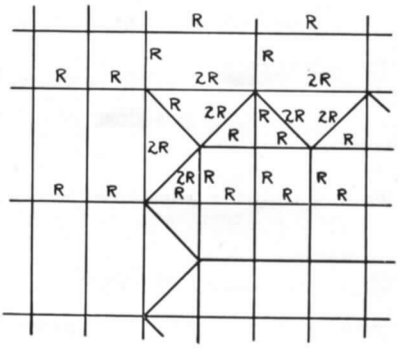

(b) Distorted scale.

FIGS. A.1a and A.1b. The network grading.

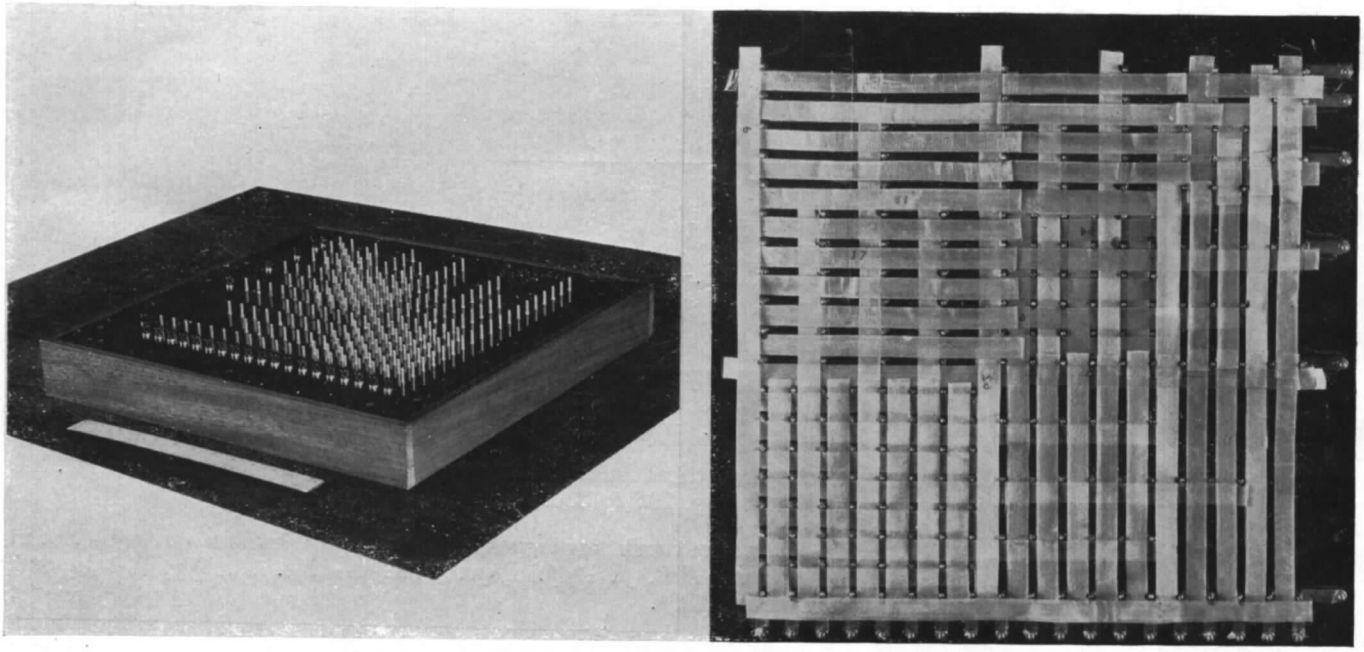

(a) Front view

(b) Rear view

FIGS. A.2a and A.2b. Graded resistance board (Grading in two directions).

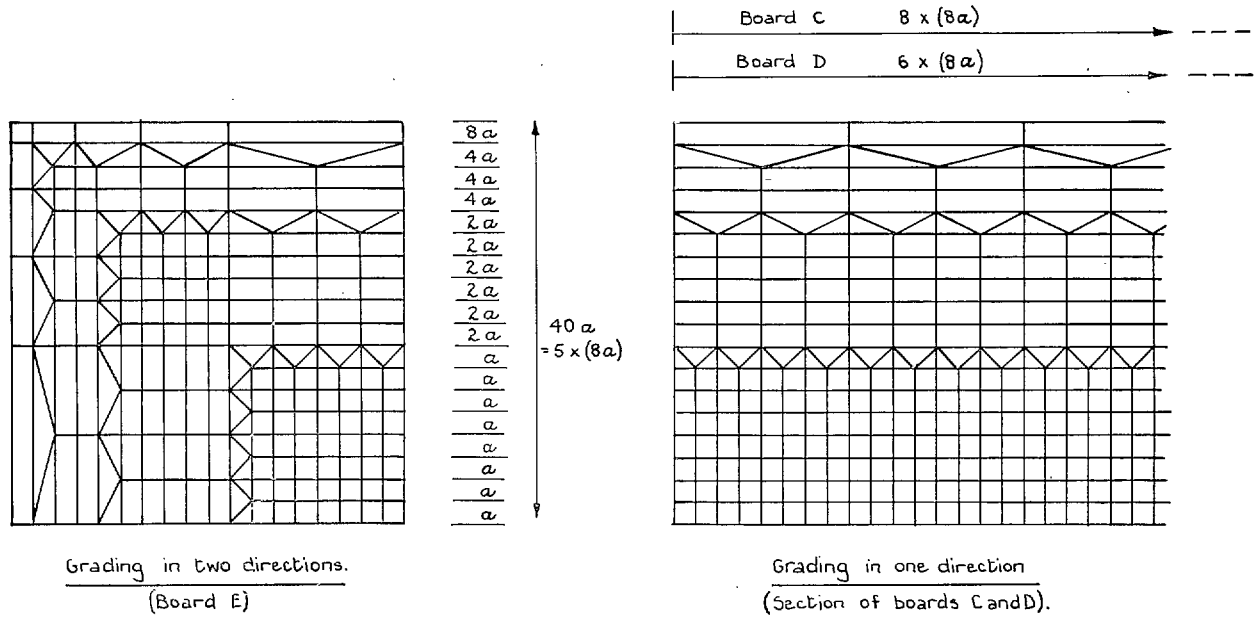

FIG. A.3. Graded resistance boards (Lay-out to distorted scale).

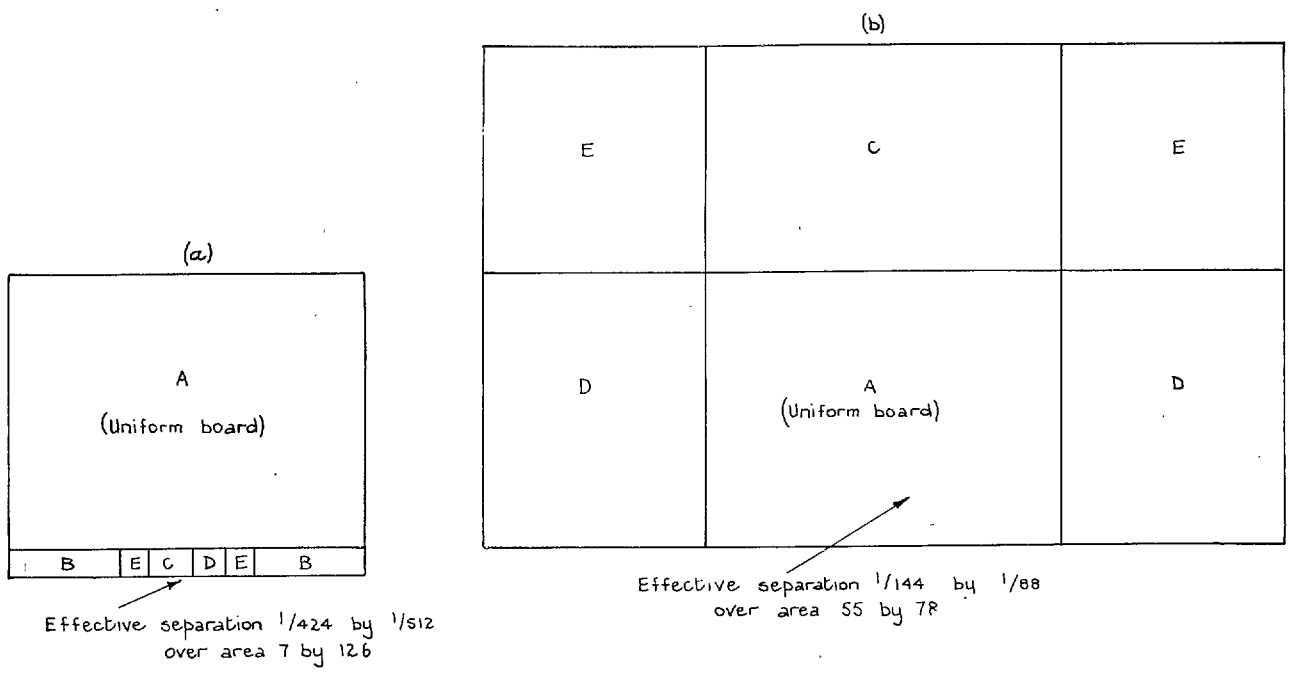

FIG. A.4. Assembled networks (Drawn to effective scale with main uniform board kept to constant size).

APPENDIX B

The Accuracy of the Electrical Resistance Network

1. *Theory.*—A theoretical solution[4] of the non-oscillatory potential problem is derived, so that detailed comparisons between theory and experiment may be made. This solution may be used to give a theoretical answer to the oscillatory problem, which was first enunciated by Glauert[5], and solved by him in a different manner.

Consider a two-dimensional aerofoil, of chord c, whose equation is $z = f(x)$, moving parallel to the x axis with velocity U. The leading edge is taken as the origin of co-ordinates and the z axis is vertically upwards. Making the usual assumptions of linearised theory, the boundary conditions for the perturbation velocity potential $\Phi(x, z)$ are:

(i) $\nabla^2\Phi = 0$

(ii) $\Phi(x, z) = -\Phi(x, -z)$

(iii) $\Phi(x, 0) = 0, \; x \leqslant 0$

(iv) $\Phi(x, 0) = \Phi(c, 0) = K, \; x \geqslant c$

(v) $\dfrac{\partial\Phi}{\partial z}(x, 0) = U\dfrac{df}{dx}, \; 0 < x \leqslant c$

(vi) $\Phi(x,z) \sim K\left(1 - \dfrac{\theta}{\pi}\right)$ as $|x^2 + z^2| \to \infty$,

where

$$0 \leqslant \theta \leqslant \pi, \; \tan\theta = \frac{z}{x}.$$

Let

$$\Phi(x, z) = \Phi_1(x, z) + \Phi_2(x, z), \text{ where}$$

$$\Phi_1(x, 0) = \Phi(c, 0) \text{ and } \Phi_2(x, 0) = 0, \; x \geqslant c$$

$$\frac{\partial\Phi_1}{\partial z}(x, 0) = 0, \text{ and } \frac{\partial\Phi_2}{\partial z} = U\frac{df}{dx}, \; 0 < x \leqslant c.$$

By the Schwartz-Christoffel theorem[1]:

$$\Phi_1(x, 0) = K - \frac{K}{\pi}\cos^{-1}\frac{2x - c}{c}, \; 0 \leqslant x \leqslant c$$

where

$$0 \leqslant \cos^{-1}\frac{2x - c}{c} \leqslant \pi.$$

$\Phi_2(x,z)$ can be determined for the general aerofoil $z = f(x)$. It is sufficient here to consider

$$z = Lx + Mx^2 + Nx^3, \quad 0 \leqslant x \leqslant c.$$

Using Refs. 2 and 3, $0 \leqslant x \leqslant c$,

$$\Phi_2(x, 0) = -U\sqrt{\{x(c - x)\}}\left[L + M\left(x + \frac{c}{2}\right) + N\left(x^2 + \frac{xc}{2} + \frac{3c^2}{8}\right)\right].$$

Therefore

$$\Phi(x, 0) = K - \frac{K}{\pi}\cos^{-1}\frac{2x - c}{c} - U\sqrt{\{x(c - x)\}}\left[L + M\left(x + \frac{c}{2}\right) + N\left(x^2 + \frac{xc}{2} + \frac{3c^2}{8}\right)\right],$$

which gives theoretical values for compiling Figs. B.2, B.3, and B.4.

By the Kutta-Joukouski condition

$$K = -\pi U\left[\frac{Lc}{2} + \frac{3Mc^2}{4} + \frac{15Nc^3}{16}\right].$$

Hence, for a flat plate in non-oscillatory flow

$$\frac{\Phi(x, 0)}{-ULc} = \frac{\pi}{2} - \frac{1}{2}\cos^{-1}\frac{2x - c}{c} + \left[\frac{x(c - x)}{c^2}\right]^{1/2} \qquad 0 \leqslant x \leqslant c\,.$$

The acceleration potential $\phi(x, z) = U\dfrac{\partial \Phi}{\partial x}(x, z)$

Therefore

$$\frac{\phi(x, 0)}{-U^2L} = \left[\frac{c - x}{x}\right]^{1/2} \qquad 0 \leqslant x \leqslant c\,,$$

which gives theoretical values for compiling Fig. B.1.

The total lift, $z = 2\rho\int_0^c \phi(x, 0)\,dx$

$$= 2\rho U\Phi(c, 0)$$

$z = -\pi L\rho U^2 c$ for a flat plate.

In the usual notation, $L = -\tan\alpha \doteq -\alpha$ for small incidence.

2. *General Considerations.*—Experimentally, it is convenient to denote the chord of an aerofoil by the number of nodes of the network (usually called pins) at which the potentials are individually adjusted to give the required gradient. For the acceleration potential analogy, n pins correspond to a chord of $(n + \frac{1}{2})$ mesh lengths. For the velocity and oscillation potential analogies, n pins correspond to a chord of n mesh lengths.

Two principal factors appeared to affect the experimental values obtained for the lift:

(i) The number of pins in the aerofoil

(ii) The effective mesh separation along that edge of the net in which the aerofoil was placed.

3. *Flat Plates: Acceleration Potential.*—The method of calculating the incidence is given in Appendix C, and three aerofoils were chosen; two experiments of eight pins and twelve pins, were carried out on a net with a mesh separation of 1/64 × 1/48. The third, of twenty pins, was on a net with an effective mesh separation of 1/512 × 1/424. Fig. B.1 shows the resulting potential functions. The value obtained at the pin next to the leading edge was much too high in each case, and does not appear on the graph as drawn. It seems that the twelve-pin aerofoil was too large for the net. Three methods of evaluating the lift were tried:

(i) Trapezoid rule on experimental values

(ii) As (i), making a correction, based on the value of ϕ at the pin next but one to the leading edge for the square-root infinity at the leading edge

(iii) As (ii), basing the correction on the value of ϕ at the pin next to the leading edge.

The experimental values of $z/(\rho U^2 c\alpha)$ are shown below:

Aerofoil:	8 pins	12 pins	20 pins
(i)	3·258	3·738	2·798
(ii)	3·434	3·942	2·932
(iii)	4·482	4·866	3·442

Since the theoretical value is π, method (iii) is ruled out. Method (ii) seems slightly better than method (i), but this is obviously rather an unsatisfactory analogy if one wished to know the lift

on an aerofoil. However, it yields reasonable pressure distributions directly. The velocity-potential analogy described below gives a very accurate value for the lift, but the pressure distribution can only be obtained by differentiation. The latter analogy seems more promising, and it alone has been used for twisted aerofoils.

4. *Flat Plates: Velocity Potential.*—Four different aerofoils (5, 10, 15, 20 pins) and three different nets (effective mesh separation 1/48 × 1/64, 1/64 × 1/48 and 1/512 × 1/424) were chosen, and the twelve experimental values of $z/(\rho U^2 c\alpha)$ are tabulated below.

Separation:	(1/48 × 1/64)	(1/64 × 1/48)	(1/512 × 1/424)
Aerofoil chord: 5 pins	3·459	3·409	3·394
Aerofoil chord: 10 pins	3·319	3·292	3·270
Aerofoil chord: 15 pins	3·309	3·270	3·213
Aerofoil chord: 20 pins	3·435	3·270	3·194

It appears that if the aerofoil is less than 0·2 of the net, the number of pins in the aerofoil is the principal factor affecting the lift. Consequently, this should be as large as possible, but less than 0·2 of the edge of the net. The theoretical and experimental values of $\Phi(x, 0)$ over the aerofoil for 20 pins on the largest board are shown in Fig. B.2, where the solid line denotes the theoretical values. The value of the lift obtained in this case is only 1·6 per cent high which is as accurate as one could hope for.

5. *Oscillatory Flow: Flat Plate.*—Comparing the boundary conditions for the oscillation potential given in the main part of the report with those for the steady-state velocity potential on the first page of this Appendix, we see that the solution of this problem depends on the solution of the non-oscillatory velocity potential problems for the following aerofoils.

(i) $z = -\dfrac{x}{c}, \qquad 0 \leqslant x \leqslant c$

(ii) $z = -\left(\dfrac{x}{c}\right)^2, \qquad 0 \leqslant x \leqslant c$

(iii) $z = -\left(\dfrac{x}{c}\right)^3, \qquad 0 \leqslant x \leqslant c\,.$

The theoretical and experimental values obtained are shown in Figs. B.2 to B.4, where the solid line denotes the theoretical values. The agreement is not as good for the twisted aerofoils as for the flat plate.

REFERENCES.—APPENDIX B

No.	*Author*	*Title, etc.*
1	E. T. Copson	*Functions of a Complex Variable.* First edition. p. 198. Oxford University Press. 1935.
2	H. Jeffreys and B. S. Jeffreys ..	*Mathematical Physics.* Second edition. Section 14, p. 111. Cambridge University Press. 1950.
3	H. Söhngen	Die Lösungen der Integralgleichung $g(x) = \frac{1}{2\pi}\int_{-a}^{a} \frac{f(\xi)}{x-\xi}\,d\xi$ und deren Anwendung in der Tragflügeltheorie. *Die Mathematische Zeitschrift.* Vol. XLIV. pp. 245 to 266. 1939.
4	E. T. Copson	Solution of a certain potential problem. (Unpublished.)
5	H. Glauert	The force and moment on an oscillatory aerofoil. R. & M. 1242. March, 1929.

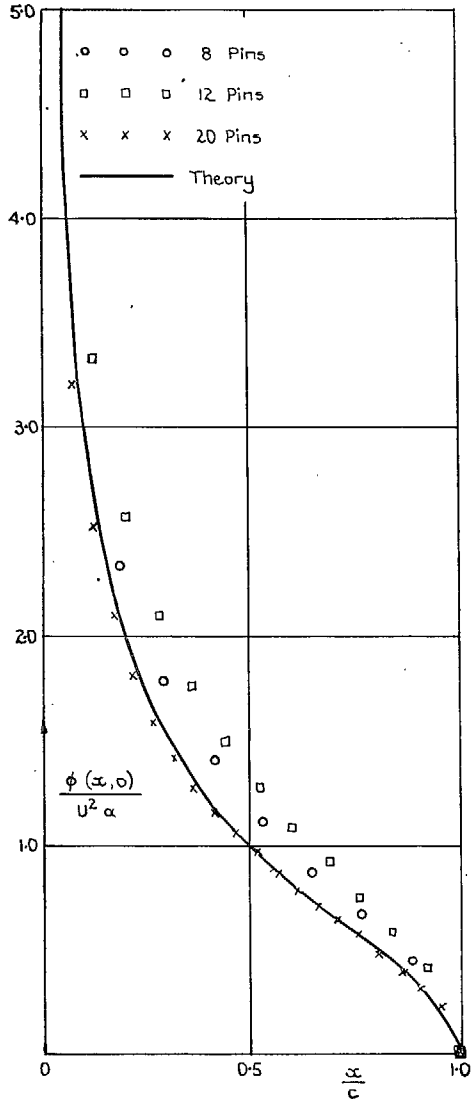

FIG. B.1.

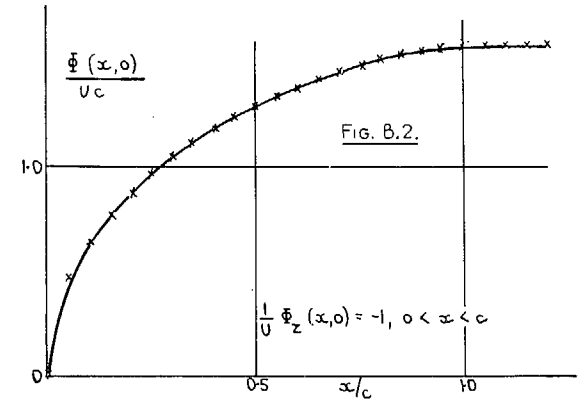

FIG. B.2.

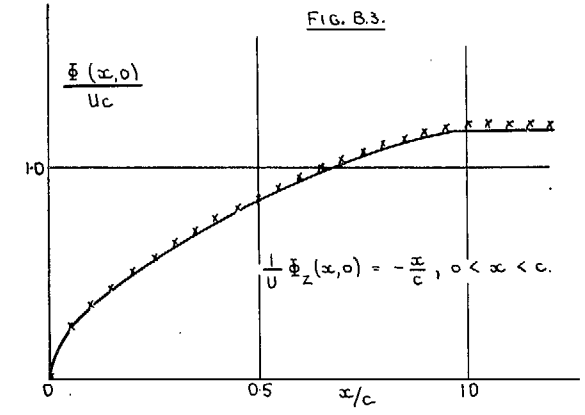

FIG. B.3.

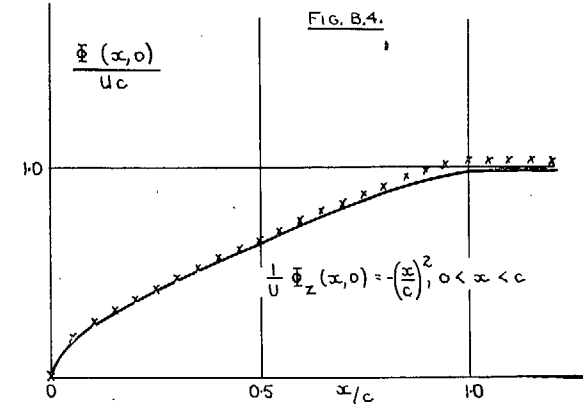

FIG. B.4.

FIGS. B.2, B.3 and B.4.

APPENDIX C

Some Details of the Procedure for Evaluating the Experimental Results

1. *Introduction.*—This Appendix considers various difficulties encountered in the course of the work and gives the methods finally selected as yielding the best results. In each case, the aerofoil is set in the centre of one edge of the net.

2. *Velocity Potential for Non-Oscillatory Flow.*—The pins in the wake were kept at a potential equal to that at the trailing edge, while the leading edge and the pins ahead of the aerofoil were kept at earth potential. The potentials over the aerofoil were adjusted so that

$$\frac{\partial \Phi}{\partial z} \equiv \frac{1}{2a}\left[-3\Phi(x, 0) + 4\Phi(x, a) - \Phi(x, 2a)\right],$$

where h is the distance between the pins. The equation of the aerofoil determines $\partial\Phi/\partial z(x, 0)$; the lift, moment and pressure on this aerofoil may then easily be calculated from $\Phi(x, 0)$.

3. *Acceleration Potential for Non-Oscillatory Flow (Flat Plates).*—In this case, the potential function is infinite at the leading edge, and the best results were obtained by considering this as half-way between two pins. The pins outside the aerofoil and at the trailing edge were earthed. That pin on the aerofoil next to the leading edge was kept at a constant potential, and $\partial\phi/\partial z$ $(x, 0)$ disregarded. The potentials at the other pins on the aerofoil were adjusted so that $\partial\phi/\partial z$ $(x, 0) = 0$ at each. The pressure difference $p(x, 0) = 2\rho\phi(x, 0)$ over the aerofoil, where the incidence α is so far unknown. In the notation of Appendix B, $L \doteq -\alpha$ when α is small.

$$U^2\alpha = -\int_{-\infty}^{x} \frac{\partial\phi}{\partial z}(\xi, 0)\, d\xi, \qquad 0 < x < c$$

$$-\int_{-\lambda c}^{x} \frac{\partial\phi}{\partial z}(\xi, 0)\, d\xi \doteq -\Sigma\, a\, \frac{\partial\phi}{\partial z}(\xi, 0), \qquad 0 < x < c$$

where $x = -\lambda c$ is the upstream edge of the board, and the sum extends from any pin on the aerofoil after the first overall upstream experimental values. From Appendix B,

$$\frac{\partial\phi}{\partial z}(\xi, 0) \to \frac{U^2 c\alpha}{2x^2} \text{ as } x \to -\infty.$$

Therefore

$$-\int_{-\infty}^{-\lambda c} \frac{\partial\phi}{\partial z}(\xi, 0)\, d\xi \doteq \frac{-U^2\alpha}{2\lambda}.$$

Beginning with the experimental value for $U^2\alpha$, in this way a convergent series for its correct value can be obtained.

4. *Oscillatory Flow for Flat Plates.*—Integrals of the form

$$\int_{-\infty}^{0} \frac{\partial\psi}{\partial z}(x, 0)\, e^{ivx/U}\, dx$$

are required to determine completely the oscillation potential function which is described in the main part of this report. From Appendix B, it can be deduced that

$$\frac{\partial\psi}{\partial z}(x, 0) \sim (-x)^{-1/2} \text{ as } x \to 0,$$

$$\frac{\partial\psi}{\partial z}(x, 0) \sim \frac{-K}{\pi x} \text{ as } x \to -\infty.$$

Filon[1] considers integrals of the form $\int_a^b \sin kx\ \psi(x)\ dx$ and gives the following formula:

$$\int_a^b \sin kx\ \psi(x)\ dx = h\{\alpha[\psi(a)\cos ka - \psi(b)\cos kb] + \beta s_{2n} + \gamma s_{2n-1}\}$$

where the interval (a, b) is divided into an even number, $2n$, of equal parts h and $kh = \theta$. Then

$$\alpha = \frac{1}{\theta} + \frac{\cos\theta\sin\theta}{\theta^2} - \frac{2\sin^2\theta}{\theta^3}$$

$$\beta = 2\left[\frac{1+\cos^2\theta}{\theta^2} - \frac{2\sin\theta\cos\theta}{\theta^3}\right]$$

$$\gamma = 4\left[\frac{\sin\theta}{\theta^3} - \frac{\cos\theta}{\theta^2}\right].$$

Also,

$$s_{2n} = \sum_{r=0}^{n} \psi(x_{2r})\sin kx_{2r} - \tfrac{1}{2}[\psi(a)\sin ka + \psi(b)\sin kb]$$

$$s_{2n-1} = \sum_{r=1}^{n} \psi(x_{2r-1})\sin kx_{2r-1}\,.$$

Filon adapts this to the case of $\int_0^\infty \frac{\phi(x)}{x}\sin kx\ dx$ and this approach is easily extended to the type of integral required. For small x, suppose $\partial\psi/\partial z\ \ (x, 0) = \tau_0/\sqrt{-x}$. This paper is interested in comparatively small frequencies, where α is negligible. Filon's formula becomes

$$\int_{-b}^{0} \frac{\partial\psi}{\partial z}\,(x, 0)\sin\frac{\nu x}{U}\,dx = \tau_0\int_{-b}^{0}\frac{\sin \nu x/U}{\sqrt{-x}}\,dx + h[\beta s_{2n} + \gamma s_{2n-1}]\,,$$

where

$$s_{2n} = \sum_{r=1}^{n}\mu_{2r}\sin 2r\theta - \tfrac{1}{2}\mu_{2n}\sin 2n\theta - \tau_0\sum_{r=1}^{n}\frac{\sin 2r\theta}{\sqrt{(2rh)}} + \frac{\tau_0\sin 2n\theta}{2\sqrt{(2nh)}}$$

$$s_{2n-1} = \sum_{r=1}^{n}\mu_{2r-1}\sin(2r-1)\theta - \tau_0\sum_{r=1}^{n}\frac{\sin(2r-1)\theta}{\sqrt{(2rh)}}$$

and

$$\frac{\partial\psi}{\partial z}\,(-rh, 0) = \mu_r\,.$$

Similarly

$$\int_{-b}^{0} \frac{\partial\psi}{\partial z}\,(x, 0)\cos\frac{\nu x}{U}\,dx = \tau_0\int_{-b}^{0}\frac{\cos \nu x/U}{\sqrt{-x}}\,dx + h[\beta s_{2n} + \gamma s_{2n-1}]\,,$$

where

$$s_{2n} = \sum_{r=1}^{n}\mu_{2r}\cos 2r\theta - \tfrac{1}{2}\mu_{2n}\cos 2n\theta - \tau_0\sum_{r=1}^{n}\frac{\cos 2r\theta}{\sqrt{(2rh)}} + \tau_0\frac{\cos 2n\theta}{2\sqrt{(2nh)}}$$

$$s_{2n-1} = \sum_{r=1}^{n}\mu_{2r-1}\cos(2r-1)\theta - \tau_0\sum_{r=1}^{n}\frac{\cos(2r-1)\theta}{\sqrt{\{(2r-1)h\}}}\,.$$

If b is chosen such that for $x \leqslant -b$, $\partial\psi/\partial z\ \ (x, 0) = -K/(\pi x)$ to the accuracy of the experiments.

$$\int_{-\infty}^{-b}\frac{\partial\psi}{\partial z}\,(x, 0)\,e^{ivx/U}\,dx = \int_{-\infty}^{-b}\frac{-K}{\pi x}\,e^{ivx/U}\,dx\,.$$

The values of $\int_{-b}^{0}\frac{e^{ivx/U}}{\sqrt{-x}}\,dx$ and $\int_{-\infty}^{-b}\frac{e^{ivx/U}}{x}\,dx$ may be found from Refs. 2 and 3.

5. *Control Surfaces.*—Much of the mathematics in the present treatment of oscillatory flow depends on the relationship

$$\bar{\Phi}(x, z) = \frac{1}{U}\int_{-\infty}^{x} \bar{\phi}(\xi, z)\, e^{\{iv(\xi - x)\}/U}\, d\xi ,$$

which is not true when the aerofoil has a sharp corner, as for a control surface. It is true, however, if the corner is rounded off as in Fig. C.1.

In the notation of the Figure,

$$0 \leqslant x \leqslant b\cos\alpha - \varepsilon\tan\frac{\beta}{2}\cos\alpha , \qquad f(x) = -h - x\tan\alpha$$

$$b\cos\alpha - \varepsilon\tan\frac{\beta}{2}\cos\alpha \leqslant x \leqslant b\cos\alpha + \varepsilon\tan\frac{\beta}{2}\cos(\alpha+\beta)$$

$$f(x) = -h - b\sin\alpha + \varepsilon\tan\frac{\beta}{2} - \varepsilon\cos\alpha + \left[\varepsilon^2 - \left(x - b\cos\alpha + \varepsilon\tan\frac{\beta}{2}\cos\alpha + \varepsilon\sin\sin a\right)^2\right]^{1/2}$$

$$b\cos\alpha + \varepsilon\tan\frac{\beta}{2}\cos(\alpha+\beta) \leqslant x \leqslant b\cos\alpha + (c-b)\cos(\alpha+\beta)$$

$$f(x) = -h - b\sin\alpha - (x - b\cos\alpha)\tan(\alpha+\beta) .$$

The experiments are arranged such that the hinge lies on a pin, and ε is taken to be so small that no other pin lies on the circular arc.

Then for small α, β

$0 \leqslant x < b$,

$$\frac{\partial\psi}{\partial z}(x, 0) = -\alpha - \frac{iv}{U}(h + 2x\alpha) + \frac{v^2}{U^2}\left(hx + \frac{x^2\alpha}{2}\right) + \frac{iv}{U}\int_{-\infty}^{0}\frac{\partial\psi}{\partial z}(x, 0)\, e^{ivx/U}\, dx$$

$$\frac{\partial\psi}{\partial z}(b, 0) = -\alpha - \frac{\beta}{2} - \frac{iv}{U}(h + 2ba) + \frac{v^2}{U^2}\left(hb + \frac{b^2\alpha}{2}\right) + \frac{iv}{U}\int_{-\infty}^{0}\frac{\partial\psi}{\partial z}(x, 0)\, e^{ivx/U}\, dx$$

$b < x \leqslant c$,

$$\frac{\partial\psi}{\partial z}(x, 0) = -\alpha - \beta - \frac{iv}{U}[h + 2x\alpha + 2(x-b)\beta] + \frac{v^2}{U^2}\left[hx + \frac{x^2\alpha}{2} + \frac{(x-b)^2\beta}{2}\right] + \frac{iv}{U}\int_{-\infty}^{0}\frac{\partial\psi}{\partial z}(x, 0)\, e^{ivx/U}\, dx .$$

REFERENCES.—APPENDIX C

No.	*Author*	*Title, etc.*
1	L. N. G. Filon	On a quadrature formula for trigonometric integrals. *Proc. Roy. Soc. E.* Vol. XLIX. pp. 38 to 47. 1928/29.
2	Anon	*Tables of sine, cosine and exponential integrals.* U.S.A. Work Projects Administration Pub. 1940 and 1942.
3	Jahnke and Emde..	*Tables of Higher Functions.* 4th edition. pp. 35 to 36. Liepzig, 1948.

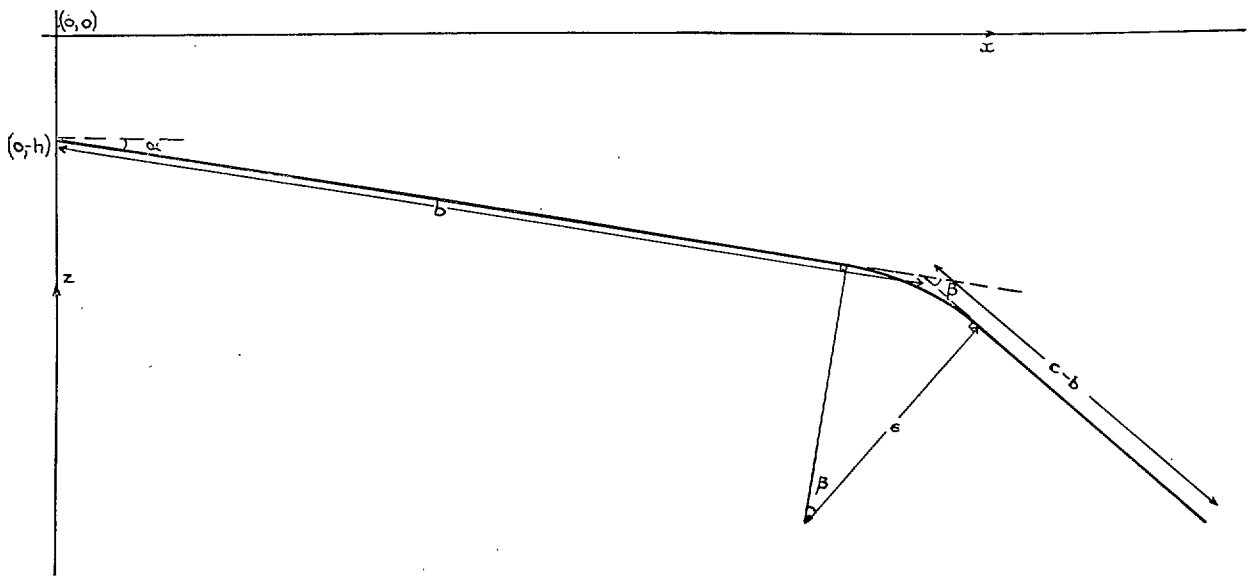

FIG. C.1.

(74988) Wt. 53/2293 K.7 9/59 Hw.

PRINTED IN GREAT BRITAIN

Publications of the Aeronautical Research Council

ANNUAL TECHNICAL REPORTS OF THE AERONAUTICAL RESEARCH COUNCIL (BOUND VOLUMES)

1939 Vol. I. Aerodynamics General, Performance, Airscrews, Engines. 50*s.* (52*s.*).
Vol. II. Stability and Control, Flutter and Vibration, Instruments, Structures, Seaplanes, etc. 63*s.* (65*s.*)

1940 Aero and Hydrodynamics, Aerofoils, Airscrews, Engines, Flutter, Icing, Stability and Control, Structures, and a miscellaneous section. 50*s.* (52*s.*)

1941 Aero and Hydrodynamics, Aerofoils, Airscrews, Engines, Flutter, Stability and Control, Structures. 63*s.* (65*s.*)

1942 Vol. I. Aero and Hydrodynamics, Aerofoils, Airscrews, Engines. 75*s.* (77*s.*)
Vol. II. Noise, Parachutes, Stability and Control, Structures, Vibration, Wind Tunnels. 47*s.* 6*d.* (49*s.* 6*d.*)

1943 Vol. I. Aerodynamics, Aerofoils, Airscrews. 80*s.* (82*s.*)
Vol. II. Engines, Flutter, Materials, Parachutes, Performance, Stability and Control, Structures. 90*s.* (92*s.* 9*d.*)

1944 Vol. I. Aero and Hydrodynamics, Aerofoils, Aircraft, Airscrews, Controls. 84*s.* (86*s.* 6*d.*)
Vol. II. Flutter and Vibration, Materials, Miscellaneous, Navigation, Parachutes, Performance, Plates and Panels, Stability, Structures, Test Equipment, Wind Tunnels. 84*s.* (86*s.* 6*d.*)

1945 Vol. I. Aero and Hydrodynamics, Aerofoils. 130*s.* (132*s.* 9*d.*)
Vol. II. Aircraft, Airscrews, Controls. 130*s.* (132*s.* 9*d.*)
Vol. III. Flutter and Vibration, Instruments, Miscellaneous, Parachutes, Plates and Panels, Propulsion. 130*s.* (132*s.* 6*d.*)
Vol. IV. Stability, Structures, Wind Tunnels, Wind Tunnel Technique. 130*s.* (132*s.* 6*d.*)

Annual Reports of the Aeronautical Research Council—

1937 2*s.* (2*s.* 2*d.*) 1938 1*s.* 6*d.* (1*s.* 8*d.*) 1939–48 3*s.* (3*s.* 5*d.*)

Index to all Reports and Memoranda published in the Annual Technical Reports, and separately—

April, 1950 - - - - R. & M. 2600 2*s.* 6*d.* (2*s.* 10*d.*)

Author Index to all Reports and Memoranda of the Aeronautical Research Council—

1909—January, 1954 R. & M. No. 2570 15*s.* (15*s.* 8*d.*)

Indexes to the Technical Reports of the Aeronautical Research Council—

December 1, 1936—June 30, 1939	R. & M. No. 1850	1*s.* 3*d.* (1*s.* 5*d.*)
July 1, 1939—June 30, 1945	R. & M. No. 1950	1*s.* (1*s.* 2*d.*)
July 1, 1945—June 30, 1946	R. & M. No. 2050	1*s.* (1*s.* 2*d.*)
July 1, 1946—December 31, 1946	R. & M. No. 2150	1*s.* 3*d.* (1*s.* 5*d.*)
January 1, 1947—June 30, 1947	R. & M. No. 2250	1*s.* 3*d.* (1*s.* 5*d.*)

Published Reports and Memoranda of the Aeronautical Research Council—

Between Nos. 2251–2349	R. & M. No. 2350	1*s.* 9*d.* (1*s.* 11*d.*)
Between Nos. 2351–2449	R. & M. No. 2450	2*s.* (2*s.* 2*d.*)
Between Nos. 2451–2549	R. & M. No. 2550	2*s.* 6*d.* (2*s.* 10*d.*)
Between Nos. 2551–2649	R. & M. No. 2650	2*s.* 6*d.* (2*s.* 10*d.*)
Between Nos. 2651–2749	R. & M. No. 2750	2*s.* 6*d.* (2*s.* 10*d.*)

Prices in brackets include postage

HER MAJESTY'S STATIONERY OFFICE

York House, Kingsway, London W.C.2; 423 Oxford Street, London W.1; 13a Castle Street, Edinburgh 2; 39 King Street, Manchester 2; 2 Edmund Street, Birmingham 3; 109 St. Mary Street, Cardiff; Tower Lane, Bristol 1; 80 Chichester Street, Belfast, *or through any bookseller.*

S.O. Code No. 23-3121